21. R. C. Reid, J. M. Alonso, *Nature* **378**, 281 (1995).
22. A. Das, C. D. Gilbert, *J. Neurophysiol.* **74**, 779 (1995).
23. J. M. Alonso, L. M. Martinez, *Nature Neurosci.* **1**, 395 (1998).
24. Correlation asymmetry is defined as $(R - L)/(R + L)$, where R is the area of the right side of the peak in the cross-correlogram and L is the area of the left side (*23*).
25. M. K. Kapadia, C. D. Gilbert, G. Westheimer, *J. Neurosci.* **14**, 451 (1994).
26. L. Maffei, A. Fiorentini, S. Bisti, *Science* **182**, 1036 (1973).
27. S. Marlin, R. Douglas, M. Cynader, *J. Neurophysiol.* **69**, 2209 (1993).
28. M. Carandini, D. Ferster, *Science* **276**, 949 (1997).
29. M. V. Sanchez-Vives, L. G. Nowak, D. A. McCormick, *J. Neurosci.* **20**, 4267 (2000).
30. F. S. Chance, S. B. Nelson, L. F. Abbott, *J. Neurosci.* **18**, 4785 (1998).
31. U. T. Eysel, D. Eyding, G. Schweigart, *NeuroReport* **9**, 949 (1998).
32. M. W. Pettet, C. D. Gilbert, *Proc. Natl. Acad. Sci. U.S.A.* **89**, 8366 (1992).
33. G. C. DeAngelis, A. Anzai, I. Ohzawa, R. D. Freeman, *Proc. Natl. Acad. Sci. U.S.A.* **92**, 9682 (1995).
34. R. A. Nicoll, R. C. Malenka, *Nature* **377**, 115 (1995).
35. D. J. Linden, J. A. Connor, *Annu. Rev. Neurosci.* **18**, 319 (1995).
36. J. M. Edeline, *Prog. Neurobiol.* **57**, 165 (1999).
37. L. F. Abbott, S. B. Nelson, *Nature Neurosci.* **3**(suppl.), 1178 (2000).
38. Y.-X. Fu *et al.*, unpublished data.
39. J. T. Trachtenberg, C. Trepel, M. P. Stryker, *Science* **287**, 2029 (2000).
40. W. Singer, C. M. Gray, *Annu. Rev. Neurosci.* **18**, 555 (1995).
41. W. Bair, *Curr. Opin. Neurobiol.* **9**, 447 (1999).
42. B. Efron, R. J. Tibshirani, *An Introduction to the Bootstrap* (Chapman and Hall, New York, 1993).
43. This work was supported by grants from the Whitaker Foundation, the National Science Foundation, and the National Eye Institute. We thank the University of Michigan for kindly providing the multielectrodes.

Supporting Online Material
www.sciencemag.org/cgi/content/full/296/5575/1999/DC1
Materials and Methods

4 February 2002; accepted 6 May 2002

REPORTS

Submicrometer Ferromagnetic NOT Gate and Shift Register

D. A. Allwood, Gang Xiong, M. D. Cooke, C. C. Faulkner, D. Atkinson, N. Vernier, R. P. Cowburn*

An all-metallic submicrometer device is demonstrated experimentally at room temperature that performs logical NOT operations on magnetic logic signals. When this two-terminal ferromagnetic structure is incorporated into a magnetic feedback loop, the junction performs a frequency division operation on an applied oscillating magnetic field. Up to 11 of these junctions are then directly linked together to create a magnetic shift register.

Devices for information technology have generally been dominated by electronics. However, emerging spin-electronics, or "spintronic," technologies (*1*, *2*), which are based on electron spin as well as charge, may offer new types of devices that outstrip the performance of traditional electronics devices. Spintronic devices use magnetic moment to carry information; advantages of such devices often include low power dissipation, nonvolatile data retention, radiation hardness, and high integration densities. Although the future of spintronics might include a solid-state realization of quantum computing (*3*), the experimental observations to date of optically (*4*) and electrically (*5*) controlled magnetism, spin-polarized current injection into semiconductors (*6–8*), ferromagnetic imprinting of nuclear spins (*9*), and control of electron-nuclei spin interactions (*10*) suggest a whole range of spintronic applications. Already, spintronic hard disk drive read-heads are well established commercially, and magnetic random access memories (MRAM) look set to follow suit.

To date, two classes of spintronic device have been proposed: semiconductor and metallic. Semiconductor devices will use spin population imbalances between electrons or nuclei. Metallic devices, including hard disk read-heads and MRAM, represent information by the magnetization direction in a ferromagnetic metal such as NiFe (Permalloy) or Co. Much work has focused on writing information to this ferromagnetic element, for example, using magnetic fields from current-carrying wires and reading information using either giant magnetoresistance (*11*) or spin-dependent tunneling junctions (*12*). However, the extent to which information can be manipulated in the magnetic form has, to date, been very limited; MRAM cells, for instance, can only store information. The scope of spintronics could be greatly expanded if in addition to data storage, magnetic data bits could interact to perform some computation between being written and detected. Magnetic information has been propagated along chains of 100-nm-diameter magnetic dots (*13*) to allow signal interconnection. However, a full logic scheme will require the development of magnetic structures that perform basic logic operations, including NOT gates for inversion operations. Such structures will form the building blocks of magnetic logic devices that perform operations analogous to current microelectronics.

Under low–magnetic field conditions, the magnetization direction within submicrometer ferromagnetic planar wires tends to lie along the wire long-axis owing to strong magnetic shape anisotropy. When two oppositely directed magnetizations meet within a wire, the realignment of successive atomic magnetic moments is not abrupt but occurs gradually over a certain distance to form a domain wall. For the 200-nm-wide, 5-nm-thick Permalloy ($Ni_{80}Fe_{20}$) wires investigated here, we calculate, using micromagnetic software (OOMMF) (*14*), that domain walls should be ~100 nm wide. It is now known that domain walls can propagate along straight submicrometer magnetic wires by application of a magnetic field parallel to the wire (*15*). A magnetic field with a vector that rotates with time in the sample plane can be used to propagate domain walls along magnetic wires that change direction and turn corners. The clockwise or counterclockwise rotation defines the magnetic field chirality, or handedness. A domain wall should propagate around a magnetic wire corner providing that the field and corner are of the same chirality. However, the chirality of a corner depends on the direction of domain wall propagation so that, within a rotating magnetic field of given chirality, a domain wall will only be able to pass through a given corner in one direction. This applies for domain walls with adjacent magnetizations either converging or diverging and satisfies the important requirement of any logic system that a definite signal flow direction must exist.

The two stable magnetization directions within submicrometer magnetic wires provide a natural means of representing the two Boolean logic states, 1 and 0. However, if there is a 180° bend in a magnetic wire and magnetization is continuous throughout, the absolute direction of magnetization will be different before and after the bend. Care must be taken in assigning logical states to different magnetization directions to avoid confusion in such situations. Therefore, we assign logical 1 to wire magnetization being in the same direction as domain wall motion and logical 0 to the magnetization direction opposing domain wall motion. Using this defi-

Department of Physics, University of Durham, Rochester Building, Science Laboratories, South Road, Durham DH1 3LE, UK.

*To whom correspondence should be addressed. E-mail: r.p.cowburn@durham.ac.uk

nition and a rotating magnetic field allows unambiguous representation of logical states.

Until now, magnetic NOT gates have proven elusive, but our structure (Fig. 1A) overcomes these difficulties and demonstrates NOT-gate functionality in a suitable rotating magnetic field. Suppose an in-plane magnetic field is rotating in a counterclockwise sense, with orthogonal components H_x and H_y (Fig. 1A). A domain wall arriving at terminal P (Fig. 1B) of the junction will propagate around the first corner of the junction (Fig. 1C) and through to terminal Q as the applied field rotates from the direction of H_x to H_y. The magnetization between P and Q will now be continuous (Fig. 1D). Then, as the magnetic field vector continues to rotate toward the direction of $-H_x$, the domain wall should propagate around the second corner of the junction (Fig. 1E), exiting at terminal R and restoring continuous magnetization between Q and R. The magnetization of the wire immediately after the junction should now be reversed compared with that immediately before the junction. The junction should therefore perform the desired NOT function with a half–field cycle propagation delay.

We have fabricated structures that incorporate this junction from 5-nm-thick Permalloy films by focused ion beam (FIB) milling (*16*). Magnetization analysis is performed at room temperature with a magneto-optical Kerr effect (MOKE) magnetometer (*17*) and averaging data over successive magnetic field cycles for several minutes. Although the focused laser-spot diameter is 5 μm, the magnetometer is sufficiently sensitive to detect magnetization reversal in a single nanowire within the laser spot and allows us to probe the magnetization of different parts of an extended structure.

Figure 2A shows a FIB image of a structure incorporating a NOT gate junction, and Fig. 2B shows a higher magnification image of the junction region. For testing purposes, a continuous input is provided to the NOT gate by feeding back the output magnetization around the structure's four-sided loop (Fig. 2A). If the magnetic junction performs an inverting function, it is a topological requirement that there should always be at least one domain wall within the ring structure, and the need for external input of a domain wall is removed. The NOT-gate input and output (indicated by I and II in Fig. 2A) were monitored by MOKE magnetometry (Fig. 2C) during application of a counterclockwise rotating magnetic field, which causes domain walls to propagate around the ring structure in a counterclockwise direction. Each MOKE trace has two levels, representing the two directions of magnetization lying parallel to the horizontal wires, and sharp transitions between these two levels, corroborating our expectation that magnetization reversal would be mediated by rapid domain wall propagation (*18*). The logical NOT behavior of the magnetic junctions is demonstrated by comparing the two MOKE traces. The output magnetization (Fig. 2C, trace II) is inverted and delayed by the expected half-cycle propagation time with respect to the input magnetization (Fig. 2C, trace I). Furthermore, the NOT gate and feedback loop are seen to be oscillating at one-third of the field frequency, i.e., the magnetic circuit is behaving as a frequency divider. This functionality is consistent with the existence of a single domain wall that experiences a half-cycle delay due to the NOT gate and a full-cycle delay due to propagation around the feedback loop. Thus, the magnetization at any point will be reversed after 3/2 field cycles and undergo full switching every 3 cycles.

Although the definite chirality of the applied field distinguishes the gate's input from its output, the high symmetry of the gate means that the input and output can readily be exchanged by reversing the applied-field chirality. We verified that on doing so, traces I and II exchanged places, proving that the direction of domain wall propagation around the magnetic ring had been reversed.

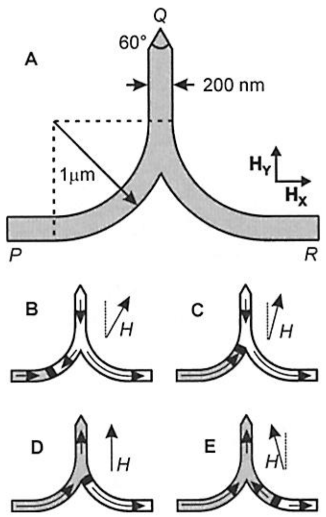

Fig. 1. (**A**) Schematic of an all-metallic ferromagnetic NOT gate and directions of elliptical magnetic field components, H_x and H_y. (**B** to **E**) Diagrams describing the operating concept of NOT-gate magnetization reversal by illustrating successive magnetization directions (arrows) and domain wall positions (thick line) within a NOT gate that undergoes domain wall injection and is subject to a rotating magnetic field.

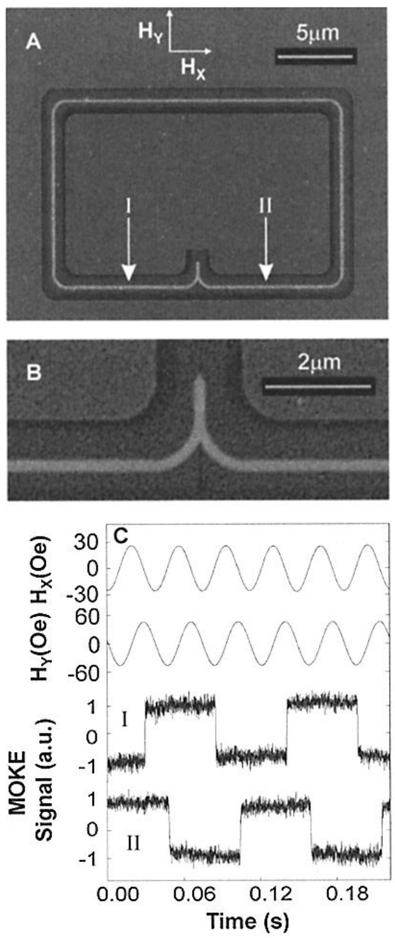

Fig. 2. (**A**) FIB image of magnetic ring, including one NOT junction. Fabrication is by FIB milling of thermally evaporated Permalloy films on silicon substrates. Thirty–kiloelectron volt Ga^+ ions, 10-pA beam current, and a focused spot diameter of 10 nm are used to fabricate wire structures of 200-nm width. Wire corners have a turning radius of 1 μm. Only the bright white shade corresponds to the magnetic material; all other contrast is due to the multistep milling process. Also indicated are the positions at which subsequent MOKE analysis was performed and the directions of elliptical magnetic field components, H_x and H_y. (**B**) High-magnification FIB image of a magnetic NOT junction. (**C**) MOKE traces from the input (trace I) and output (trace II) of the NOT junction [indicated in (A)] within a counterclockwise rotating magnetic field (H_x = 25 Oe and H_y = 46 Oe). The typical differential Kerr signal obtained from 200-nm-wide, 5-nm-thick Permalloy wires is dI/I = 0.025%. The MOKE magnetometer uses a continuous-wave Nd:VO_3 laser (532-nm operating wavelength) and an XYθ stepper-motor sample mount. Lock-in amplification of the MOKE signal during a two-dimensional raster scan of the sample allows a magnetic susceptibility map to be generated, permitting different sections of a sample to be selected for analysis. During fabrication, a 100 μm by 100 μm area of film around the structure is removed by using a number of different FIB currents in the range 100 pA to 20 nA to render negligible the contribution of the surrounding magnetic film to the optical magnetometry signal.

Although these observations support the general operating concept shown in Fig. 1, B to E, we do not yet know how a domain wall transfers from the input arm of a NOT gate to its output arm (Fig. 1, C and D). Possible mechanisms include rotation of the domain wall around the central NOT-gate arm, bending and splitting of the domain wall, or a more complex mechanism in which the simple geometry of a domain wall breaks down. Initial micromagnetics simulations suggest the latter, highlighting how the use of macroscopic concepts such as domain walls can sometimes be inappropriate in submicrometer magnetic structures.

Directly linking logic gates has not been possible with previously proposed reconfigurable magnetic logic systems (*19*, *20*) where a sequential magnetic-electronic-magnetic conversion of logic levels is required between successive elements. To demonstrate that our logic gates can be concatenated without converting back to electronic signals between gates, we have fabricated a magnetic ring structure containing a chain of three magnetic NOT gates (Fig. 3A), each separated by a 1-μm wire length. The results of applying a counterclockwise rotating magnetic field are shown in Fig. 3B. The MOKE traces repeat every five magnetic field cycles, consistent with half-period propagation delays per NOT gate and one cycle for the feedback loop. However, we were able to obtain two different bit patterns from the same MOKE measurement point, depending on the starting conditions of the circuit. In both cases, the gates were initialized by the application of a magnetic field (150 Oe) pulse followed by a sinusoidal magnetic field of reducing amplitude, both in the direction of H_y (Fig. 3A). The pulse was used to align the magnetization of all wire sections parallel to H_y and the second, demagnetizing field to randomly annihilate adjacent domain walls (*21*). This provides us with a limited number of distinct bit patterns. MOKE trace I (Fig. 3B) has the simplest bit pattern, with only two transitions per period, similar to the one-gate ring above (Fig. 2C); this represents a single domain wall propagating around the ring. MOKE trace II (Fig. 3B), however, has six transitions per period, which is consistent with the existence of three domain walls. Although the initial pattern selection was random, once chosen, the pattern persisted within the ring for the several thousand field cycles applied during testing. By not using the demagnetizing field before MOKE analysis, we have also obtained MOKE traces with 10 transitions per period, which corresponds to the circulation of five domain walls.

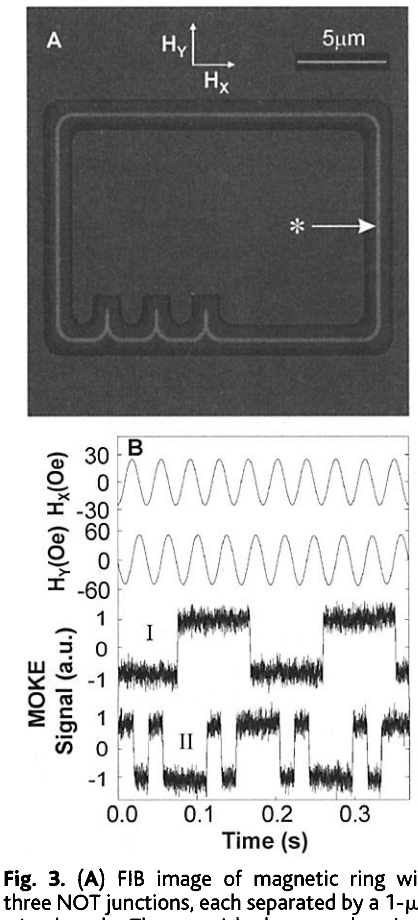

Fig. 3. (**A**) FIB image of magnetic ring with three NOT junctions, each separated by a 1-μm wire length. The asterisk denotes the single position of subsequent MOKE. The directions of elliptical magnetic field components, H_x and H_y, are also indicated. (**B**) Two MOKE traces (I and II) from a magnetic ring with three NOT junctions within a counterclockwise rotating magnetic field (H_x = 25 Oe and H_y = 50 Oe), demonstrating propagation of one and three domain walls around the ring, respectively.

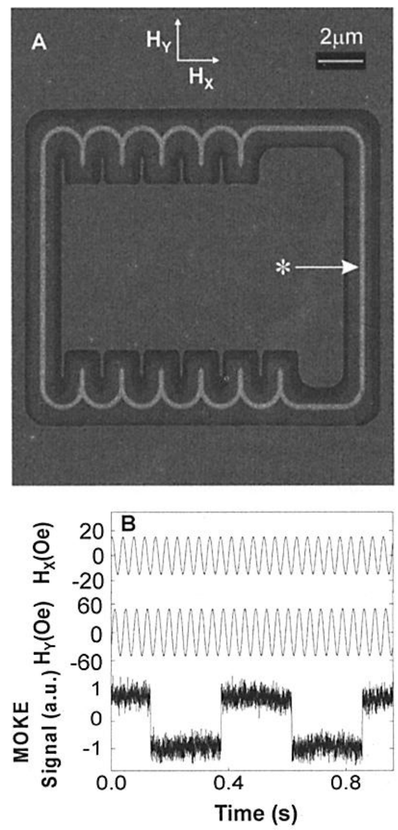

Fig. 4. (**A**) FIB image of a magnetic ring including 11 NOT junctions, with the asterisk indicating the position of subsequent MOKE analysis. The directions of elliptical magnetic field components, H_x and H_y, are also indicated. (**B**) MOKE analysis of an identical structure within a clockwise-rotating magnetic field (H_x = 15 Oe and H_y = 50 Oe).

Figure 3B demonstrates, therefore, that logical information can be passed directly from one NOT gate to another. This is a key step toward powerful, multistep logic functionality in ferromagnetic systems. Furthermore, the device shown in Fig. 3A is actually a 5-bit serial shift register, made up of 1 bit per NOT gate and 2 bits for the feedback loop; the fact that a complex bit pattern was preserved during cycling shows that each bit of the shift register may be given an independent value. The motion of a domain wall along a chain of magnetic NOT gates under the action of a rotating magnetic field exhibits some similarities with data circulation in magnetic bubble shift register memories (*22*).

The NOT gates and shift registers described above have all shifted data in one direction only. A fully flexible magnetic logic architecture must be able to process data flowing in different directions on the same chip. We have therefore fabricated a magnetic ring containing 11 NOT gates (Fig. 4A), of which 6 shift data in one direction and 5 shift data in the other direction. The latter are obtained simply by reflecting the junction in the horizontal axis so that the chirality of its arms remains matched to the applied field chirality. The MOKE results obtained during application of a clockwise rotating field are shown in Fig. 4B. The ring structure switches with a period of 13 field cycles, showing that all gates are working and that the data are cycling correctly through this 13-bit shift register (1 per NOT gate plus 2 for the feedback loop).

To test the repeated operation of a shift register, we acquired the data in Fig. 4B over 30 min of cycling. This corresponds to the same single domain wall undergoing ~100,000 NOT operations. The observation of a strong signal with very sharp transitions (Fig. 4B) shows that all of these NOT operations were performed correctly; failure of even a single operation would have broken the coherence of the data averaging, leading to smearing of the sharp transitions. Although this is not a full engineering test of bit error rates, it is an indication that these devices are not as sensitive to the problems of 360° domain wall build-up and irreproducible magnetic switching as other spintronic devices have been.

The operational frequency demonstrated

throughout this study is only 27 Hz, but this can be attributed to our use of an iron-cored electromagnet to apply the rotating field. If these devices were mounted on a high-frequency stripline, operating speed would ultimately be limited by the domain wall propagation time through a single gate. For domain wall mobility, $\mu = 30\ \mathrm{ms^{-1}\ Oe^{-1}}$ (*23*), and current experimental conditions, we calculate an operating frequency of >200 MHz for devices with a 1-μm radius of curvature. This operating frequency will increase as the size of the gate is further reduced. We estimate the switching energy of the magnetic NOT gates presented here to be 35 eV per transition (*24*) (1400kT, where k is Boltzmann's constant and T is room temperature), indicating very great stability of data against thermal loss.

A particularly interesting feature of these NOT gates is that they can perform real logic operations on real data without the use of any semiconductor material. This makes scaling to the nanoscale very simple: first, because of the much higher carrier density in metals than in semiconductors; and second, because of the lack of multilayer heterostructures requiring precise alignment. Domain wall widths should not limit this miniaturization because we expect their value to decrease with track widths, tending to the exchange length (5 nm for Permalloy) as track widths approach the film thickness. However, it is currently unclear whether miniaturization will cause appreciable domain wall pinning at defects.

Three further logic elements are required in addition to the NOT gate and shift register described here in order to make a fully universal logic architecture. These are a two-input logic gate that performs an AND, OR, or XOR function; a fan-out structure that converts one domain wall into two walls; and a structure that allows magnetic tracks to cross over each other. An advantage of the rotating clock field is that domain walls move in orthogonal directions at different times. Consequently, it may be possible to cross two tracks in the same plane without interference of the magnetic signals. Domain wall replication should be possible by simply splitting a magnetic track into two branches. The extra energy needed to create the second domain wall comes from the work done by the applied magnetic field against the domain wall pinning force at the junction. The opposite structure, in which two tracks feed into one, may by used to achieve the two-input logic function, using the wire-OR method from microelectronics. In this case, some magnetic biasing will also be required, analogous to the pull-up resistor in the wire-OR scheme.

For a fully functioning nanomagnetic logic system, it will also be necessary to interface conventional electronic signals. Data can be written into the magnetic structures by a current-carrying stripline; and data can be read out by incorporating spin tunnel junctions or spin valves into magnetic tracks or, alternatively, by measuring domain wall resistance.

References and Notes

1. G. A. Prinz, *Science* **282**, 1660 (1998).
2. S. A. Wolf *et al.*, *Science* **294**, 1488 (2001).
3. D. Loss, D. P. DiVicenzo, *Phys. Rev. A* **57**, 120 (1998).
4. S. Koshihara *et al.*, *Phys. Rev. Lett.* **78**, 4617 (1997).
5. H. Ohno *et al.*, *Nature* **408**, 944 (2000).
6. D. J. Monsma, R. Vlutters, J. C. Lodder, *Science* **281**, 407 (1998).
7. R. Fiederling *et al.*, *Nature* **402**, 787 (1999).
8. Y. Ohno *et al.*, *Nature* **402**, 790 (1999).
9. R. K. Kawakami *et al.*, *Science* **294**, 131 (2001).
10. J. H. Smet *et al.*, *Nature* **415**, 281 (2002).
11. M. N. Baibich *et al.*, *Phys. Rev. Lett.* **61**, 2472 (1988).
12. J. S. Moodera, L. R. Kinder, T. M. Wong, R. Meservey, *Phys. Rev. Lett.* **74**, 3273 (1995).
13. R. P. Cowburn, M. E. Welland, *Science* **287**, 1466 (2000).
14. http://math.nist.gov/oommf/
15. T. Ono *et al.*, *Science* **284**, 468 (1999).
16. G. Xiong, D. A. Allwood, M. D. Cooke, R. P. Cowburn, *Appl. Phys. Lett.* **79**, 3461 (2001).
17. R. P. Cowburn, D. K. Koltsov, A. O. Adeyeye, M. E. Welland, *Appl. Phys. Lett.* **73**, 3947 (1998).
18. The magnetization transitions shown in Fig. 2C indicate that domain walls require a parallel magnetic field of just 3 Oe to propagate in continuous wire sections, which is when the orthogonal component of the rotating field is close to its maximum value.
19. W. C. Black Jr., B. Das, *J. Appl. Phys.* **87**, 6674 (2000).
20. C.-Y. You, S. D. Bader, *J. Appl. Phys.* **87**, 5215 (2000).
21. In the previous case of one NOT gate in a feedback loop, no pulsed-field initialization was required owing to the simpler topology involved.
22. W. A. Triebel, A. E. Chu, *Handbook of Semiconductor and Bubble Memories* (Prentice-Hall, Englewood Cliffs, NJ, 1982).
23. M. Redjdal, J. Guisti, M. F. Ruane, F. B. Humphrey, *J. Appl. Phys.*, **91**, 7547 (2002).
24. Switching energy was calculated with the area of the magnetization hysteresis loop and suitable bulk constants.

25. This work was supported by Eastgate Investments Ltd.

6 February 2002; accepted 19 April 2002

Ferroelectric $Bi_{3.25}La_{0.75}Ti_3O_{12}$ Films of Uniform *a*-Axis Orientation on Silicon Substrates

Ho Nyung Lee, Dietrich Hesse, Nikolai Zakharov, Ulrich Gösele

The use of bismuth-layered perovskite films for planar-type nonvolatile ferroelectric random-access memories requires films with spontaneous polarization normal to the plane of growth. Epitaxially twinned *a* axis–oriented La-substituted $Bi_4Ti_3O_{12}$ (BLT) thin films whose spontaneous polarization is entirely along the film normal were grown by pulsed laser deposition on yttria-stabilized zirconia-buffered Si(100) substrates using $SrRuO_3$ as bottom electrodes. Even though the (118) orientation competes with the (100) orientation, epitaxial films with almost pure (100) orientation were grown using very thin, strained $SrRuO_3$ electrode layers and kinetic growth conditions, including high growth rates and high oxygen background pressures to facilitate oxygen incorporation into the growing film. Films with the *a*-axis orientation and having their polarization entirely along the direction normal to the film plane can achieve a remanent polarization of 32 microcoulombs per square centimeter.

Ferroelectric bismuth-layered perovskite films are being studied for use as nonvolatile digital memories. Polycrystalline films, such as $SrBi_2Ta_2O_9$ (SBT) (*1*) and La-substituted $Bi_4Ti_3O_{12}$, including $Bi_{3.25}La_{0.75}Ti_3O_{12}$ (BLT) (*2*), are of great interest in part because of their high fatigue endurance. However, randomly oriented polycrystalline films have certain limitations, and they may have unacceptable cell-to-cell variations when the lateral size of the ferroelectric cells is below 100 nm, as is required for gigabit memories (*3*).

Conceptually, epitaxially grown films should overcome this nonuniformity problem, and numerous attempts have been made to grow thin films by pulsed laser deposition (PLD) (*4–8*) as well as other methods (*9–12*). Because of their highly anisotropic structure [$Bi_4Ti_3O_{12}$ is pseudo-orthorhombic with a = 0.545 nm, b = 0.541 nm, and c = 3.283 nm (*13*)], epitaxial thin films of these materials can easily be grown with the [001] axis perpendicular to the film plane (i.e., in the so-called c-axis orientation). However, c axis–oriented films have a negligible polarization component along the film normal, because the vector of the (major) spontaneous polarization in these layered perovskite materials is along the a axis (*13, 14*). Recent efforts have concentrated on the growth of epitaxial films with non–c-axis orientations

Max-Planck-Institut für Mikrostrukturphysik, Weinberg 2, D-06120 Halle/Saale, Germany.